



A simple rapid route to synthesize monocalcium phosphate monohydrate using calcium carbonate with different phases derived from green mussel shells

S. Seesanong¹, C. Laosinwattana¹, B. Boonchom²

¹ Department of Plant Production Technology, Faculty of Agricultural Technology, King Mongkut's Institute of Technology Ladkrabang Bangkok 10520, Thailand

² Municipal Waste and Wastewater Management Learning Center: Functional Phosphate Materials Unit, Faculty of Science, King Mongkut's Institute of Technology Ladkrabang, Bangkok 10520, Thailand

Received 13 March 2019,
Revised 28 April 2019,
Accepted 29 April 2019

Keywords

- ✓ Green mussel shells,
- ✓ Calcium carbonate,
- ✓ Monocalcium phosphate monohydrate,
- ✓ Rapid synthesis,

banjong.bo@kmitl.ac.th
Phone: 66-2329-8400
Fax: +66- 2329-8412

Abstract

Calcium carbonate with different phases was successfully prepared by a rapid simple, easily available, low-cost instrument, an environmentally benign method using only mechanical grinding process of green mussel shells. Three mixed calcium carbonate phases consisting of vaterite (87.75%), aragonite (4.40%) and calcite (7.85%), obtained from green mussel shells were used for the first time to produce monocalcium phosphate monohydrate $\text{Ca}(\text{H}_2\text{PO}_4)_2 \cdot \text{H}_2\text{O}$, which was prepared by the mechanical mixing of the as-synthesized CaCO_3 and phosphoric in aqueous-acetone media at ambient temperature with short time consumption (30 min). The as-synthesized CaCO_3 and $\text{Ca}(\text{H}_2\text{PO}_4)_2 \cdot \text{H}_2\text{O}$ products were characterized by thermal gravimetric analysis (TG/DTG), X-ray powder diffraction (XRD), FTIR spectroscopy and scanning electron microscopy (SEM). The reproducible and low-cost method suggested that it could be used in industry for the large scale synthesis of CaCO_3 and $\text{Ca}(\text{H}_2\text{PO}_4)_2 \cdot \text{H}_2\text{O}$ from green mussel shells and expected to be alternative for the removal and value-added of green mussel shells to reduce enormous wastes in the future.

1. Introduction

Calcium phosphates have attracted more attention due to plenty of potential applications in various industries as a food additive, animal feed, fertilizer, ceramic, cosmetic and medical, etc.[1-9] Among these calcium phosphates, monocalcium phosphate monohydrate $\text{Ca}(\text{H}_2\text{PO}_4)_2 \cdot \text{H}_2\text{O}$ has been extensively used as mention above. So far, the $\text{Ca}(\text{H}_2\text{PO}_4)_2 \cdot \text{H}_2\text{O}$ powders have been prepared from commercial grades of expensive chemical raw materials such as calcium nitrate, calcium chloride, calcium acetate, calcium oxalate, calcium oxide, calcium hydroxide and calcium carbonate for calcium source and ammonium dihydrogen phosphate, diammonium hydrogen phosphate and phosphoric acid for phosphorus source[13-16, 10-26]. The general synthetic methods reported need to use hard and complex procedures; chemical precipitation[3, 27, 28], the sol-gel process[10], microwave synthesis[29, 30], hydrothermal synthesis[4, 21, 23], emulsion processing[22], and mechanochemical method[15, 24]. Recently, some researchers had been studied on preparations of calcium phosphates (dicalcium phosphate, monocalcium phosphate, tricalcium phosphate and hydroxyapatite) from cockle shells[7], oyster shells[31], corbicula shells[32] and Mediterranean mussel shells[27]. However, the previously reported preparations had trouble processes due to needing to control of temperature, pH, the time-consuming and specific quantity of raw materials affected to a high cost of a product.

Recently, environmental considerations are a strong emphasis on using recycled waste materials [1, 2]. Every day billions of large green mussels' meats were consumed, so shell wastes were generated too many tons in Thailand [3]. Until now green mussel shells are being throwaway, begetting fatal environmental obstacles such as unpleasant odor, flies voice and germ source[4]. The scarcity of landfills and dumping areas took challenges to this shell waste management. Several advances hold to shift shell wastes typically aimed for a landfill, such as soil amendment, fertilizer, the additive for animal feed and food, adsorbents, brick, calcium supplement, paper manufacture, ceramic industry, etc. [5-12]. Green mussel shells roughly represent 31-33% of the mussel weight and shell consist 95-99% of calcium carbonate and 1-5% of the organic matrix [13, 14].

Therefore, shell wastes of green mussels are a smart alive source of calcium, which can be used as a choice to calcium carbonate agent from mineral source to produce various calcium compounds. Additionally, a raw material, calcium carbonate derived from green mussel shells, is inexpensive and inexhaustible natural calcium resources[14]. Furthermore, consuming green mussel shells using as calcium carbonate agent in a wide range of applications contributes to solid minimization.

The aim of this work is to prepare calcium carbonate with different phases from green mussel shells (enormous wastes and inexhaustible natural resource for using inexpensively raw material) and demonstrate that it can be used to produce monocalcium phosphate monohydrate $\text{Ca}(\text{H}_2\text{PO}_4)_2 \cdot \text{H}_2\text{O}$. The different phases of the as-synthesized CaCO_3 obtained from green mussel shells were calculated by Kontoyannis and Vagenas equation and were used to react with phosphoric acid in aqueous-acetone media at ambient temperature and short time consumption for preparation of $\text{Ca}(\text{H}_2\text{PO}_4)_2 \cdot \text{H}_2\text{O}$ reported for the first time. The as-prepared compounds were characterized by thermo gravimetric-differential thermal analysis (TG/DTG/DTA), X-ray diffraction (XRD), Fourier transform-infrared spectroscopy (FTIR) and scanning electron microscopy (SEM).

2. Material and Methods

In this study, calcium carbonate (CaCO_3) was prepared by green mussel shells taken from Thailand. Approximately 500 g of green mussel shells were washed by sodium hypochlorite to scrub and removed dirt and then dried in open air. The dried green mussel shells were finely grounded using a grinder machine. The powders were sieved using a stainless laboratory test sieve with an aperture size of 500 meshes to obtain micronized powders. The resulting powders obtained from green mussel shells are calcium carbonate (CaCO_3). Phosphoric acid (86.4 %w/w H_3PO_4 , Merck) and $\text{CH}_3\text{CH}_2\text{OCH}_2\text{CH}_3$ (98 % v/v; Merck) were used as starting materials without further purification. Deionized water was used throughout the experiment. In a typical synthetic procedure of $\text{Ca}(\text{H}_2\text{PO}_4)_2 \cdot \text{H}_2\text{O}$, 100 mL of acetone was poured into 100.00 g of CaCO_3 powders and then was continuously stirred with a magnetic stirrer, referred as suspension A. After that, 166 mL of 70 %w/w H_3PO_4 was slowly added to the suspension A and was vigorously stirred at ambient temperature for 15 min. The resulting reaction was aged for 30 min to form the precipitates, which thereupon filtered by the suction pump, washed three times in acetone until free from phosphate ion and then dried in air for 24 h. The obtained powders were called as mono calcium phosphate monohydrate ($\text{Ca}(\text{H}_2\text{PO}_4)_2 \cdot \text{H}_2\text{O}$).

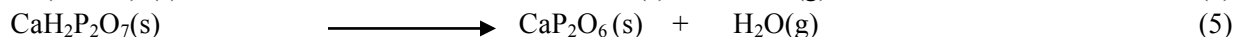
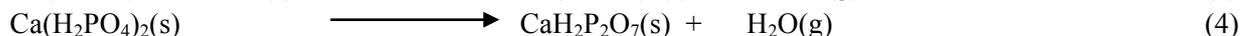
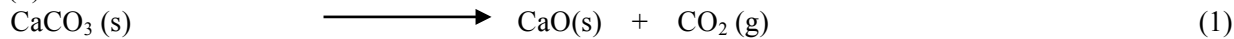
In order to determine characterization of CaCO_3 and $\text{Ca}(\text{H}_2\text{PO}_4)_2 \cdot \text{H}_2\text{O}$, calcium contents were determined by atomic absorption spectrophotometry (AAS, Perkin Elmer, Analyst100). The phosphorus content was determined by colorimetric analysis of the molybdophosphate complex. The water content was analyzed by TG data investigated on a TG-DTA Pyris Diamond Perkin-Elmer Instruments. Phase analysis of samples were conducted using X-ray diffraction (XRD) (PW3710, The Netherlands) with $\text{Cu K}\alpha$ radiation ($\lambda = 0.15406$ nm). FTIR spectra of as-prepared samples were recorded by a Perkin-Elmer Spectrum GX FT-IR/FT-Raman spectrometer in the range of $4000\text{-}370$ cm^{-1} with 8 scans and the resolution of 4 cm^{-1} using KBr pellets (KBr, spectroscopy grade, Merck). The morphologies of the selected resulting samples were examined with Scanning Electron Microscope (SEM) using LEO SEM VP1450 after gold coating.

3. Results and discussion

The calcium content of the as-synthesized CaCO_3 determined by atomic absorption spectrophotometry (AAS), found to be 39.93 wt% Ca_{total} , which is close to the theoretical values (39.97% Ca) for CaCO_3 . While the calcium and phosphorus contents of the as-synthesized $\text{Ca}(\text{H}_2\text{PO}_4)_2 \cdot \text{H}_2\text{O}$ determined by colorimetric analysis of the molybdophosphate complex and AAS, respectively, found to be 15.45 wt% Ca_{total} and 24.02 wt% P_{total} , suggesting the molar ratio $\text{Ca}_{\text{total}} : \text{P}_{\text{total}} = 1.00:2.00$ [29]. The water content was analyzed by TG data (Figure 1) and was about of 22.88 wt% (3.20 mol) H_2O . These results indicate that the prepared sample could be $\text{Ca}(\text{H}_2\text{PO}_4)_2 \cdot 1.20\text{H}_2\text{O}$ [29].

The results of simultaneous TG/DTG analyses of the as-synthesized CaCO_3 and $\text{Ca}(\text{H}_2\text{PO}_4)_2 \cdot \text{H}_2\text{O}$ are shown in Figures 1 and 2. The TG curve of the as-synthesized CaCO_3 (Figure 1) shows three stages of the small and large mass losses in the range of 475-500 and 550-800 $^\circ\text{C}$, which related with the respective DTG peaks: 484 and 753 $^\circ\text{C}$. The total mass loss is 44% (1 mol CO_2) and the retained mass of 56% indicated that CaO was formed, which is good agreement with the theoretical value[33]. The thermal decomposition of the as-synthesized CaCO_3 related to decarboxylation reaction shown in Eq. (1). Whereas the TG curve of the as-synthesized $\text{Ca}(\text{H}_2\text{PO}_4)_2 \cdot \text{H}_2\text{O}$ (Figure 2) shows four stages of the weight loss in the range of 100-150, 150-200, 200-250 and 250-600 $^\circ\text{C}$. These four stages appear in the respective DTG as four peaks: 127, 182, 237 and 265 $^\circ\text{C}$. The total mass loss is 22.88% (3.20 mol H_2O), which is close to the theoretical values (21.42% (3 mol H_2O) for $\text{Ca}(\text{H}_2\text{PO}_4)_2 \cdot \text{H}_2\text{O}$ [34]. The thermal decomposition of the as-synthesized $\text{Ca}(\text{H}_2\text{PO}_4)_2 \cdot \text{H}_2\text{O}$ is a complex

process, which involves the dehydration of the coordinated water molecules (1 mol H₂O) and an intramolecular dehydration of the protonated phosphate groups (2 mol H₂O), these processes could formally be presented as Eq. (2)-(5):



The new molecule (Ca(H₂PO₄)₂) and intermediate compound (CaH₂P₂O₇) have been registered. The calcium polyphosphate, CaP₂O₆ is found to be the final product of the thermal decomposition at T > 600 °C. The thermal result of the prepared compound is different from that reported in the literatures [33-35].

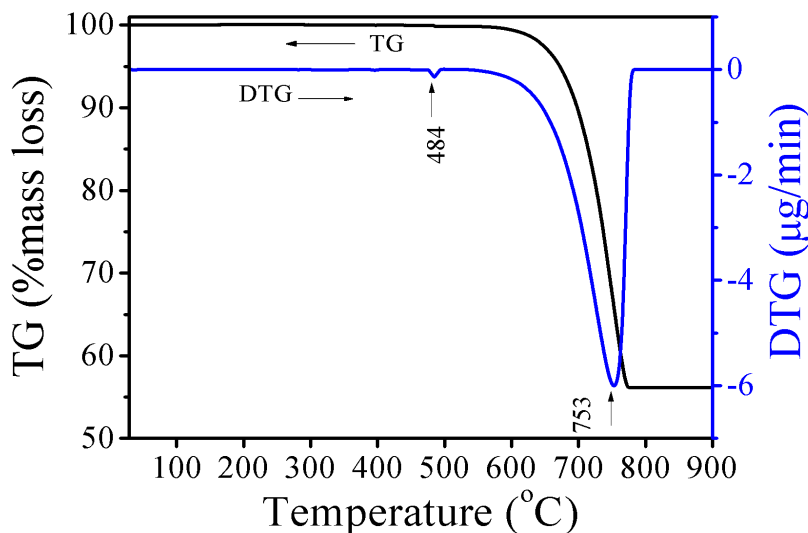


Figure 1: TG/DTG curves of the as-synthesized CaCO₃ obtained from by green mussel shells at a heating rate of 10 °C min⁻¹

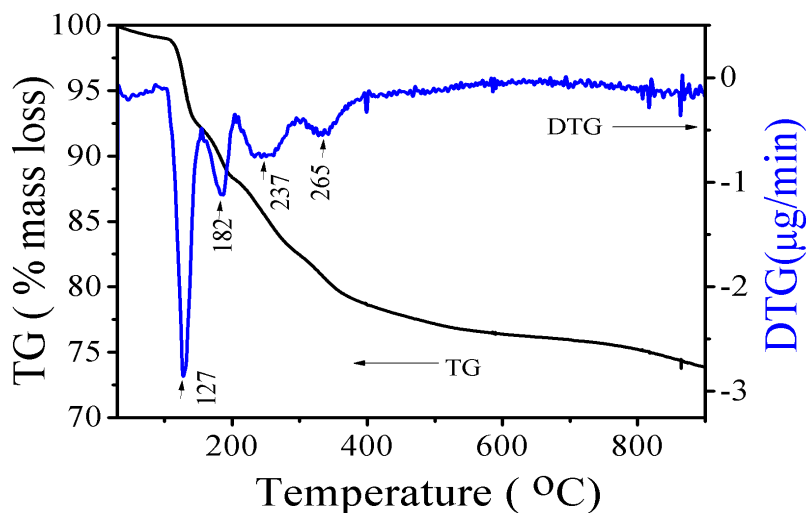


Figure 2: TG/DTG curves of the as-synthesized Ca(H₂PO₄)₂·H₂O at a heating rate of 10 °C min⁻¹.

The XRD patterns of the as-synthesized CaCO₃ and Ca(H₂PO₄)₂·H₂O powders are presented in Figure 3. The XRD peaks of the as-synthesized CaCO₃ powder were compared with the standard PDF data of the three CaCO₃ phases as calcite (PDF#72-1937), vaterite (PDF#74-1867) and aragonite (PDF#75-2230), which respectively crystallizes rhombohedral, orthorhombic and orthorhombic structures [3, 31]. The related XRD pattern shown in Figure 3 exhibits three sharp peaks at 2θ = 26.20, 29.56 and 33.22° corresponding to (111), (104) and (112) reflections and are characteristic of calcite, aragonite and vaterite phases, respectively. The XRD results indicate that the as-synthesized CaCO₃ has the mixing of three phases of calcium carbonate. The relative

percentages of different phases in the samples were estimated from the respective maximum intensity peaks employing the method reported by Kontoyannis and Vagenas [36] using the following relations (Eq.6 and 7).

mole fraction of vaterite,

$$X_V = \frac{7.69I_V^{112}}{I_c^{104} + 3.157I_A^{111} + 7.69I_V^{112}} \quad (6)$$

mole fraction of aragonite,

$$X_A = \frac{3.157I_A^{111}}{I_c^{104} + 3.157I_A^{111} + 7.69I_V^{112}} \quad (7)$$

and mole fraction of calcite, $X_C = 1 - X_V - X_A$

where I_V^{112} , I_A^{111} and I_C^{104} are the intensities of the X-ray diffraction peaks and the subscripts V, A and C represent vaterite, aragonite and calcite, respectively, and the superscripts the XRD reflection planes. The calculated percentages of different phases are found to be 87.75, 4.40, 7.85% for vaterite, aragonite and calcite, respectively. As this result, the as-prepared CaCO_3 sample is predominantly of vaterite phase with minor phases of calcite and aragonite estimated by the Kontoyannis and Vagenas equation using XRD data, which may be useful for studying natural other shells. As shown in Figure 3, this data belongs to the as-prepared $\text{Ca}(\text{H}_2\text{PO}_4)_2 \cdot \text{H}_2\text{O}$ compound and exhibits two sharp characteristic peaks at $2\theta = 22.95$ and 24.18° corresponding to (021) and (120) reflections for anorthic crystal structure of $\text{Ca}(\text{H}_2\text{PO}_4)_2 \cdot \text{H}_2\text{O}$. According to the standard data as PDF# 700090, the labeled diffraction peaks can be indexed, which confirm the as-prepared $\text{Ca}(\text{H}_2\text{PO}_4)_2 \cdot \text{H}_2\text{O}$ crystal structure is in anorthic system with space group Pt.

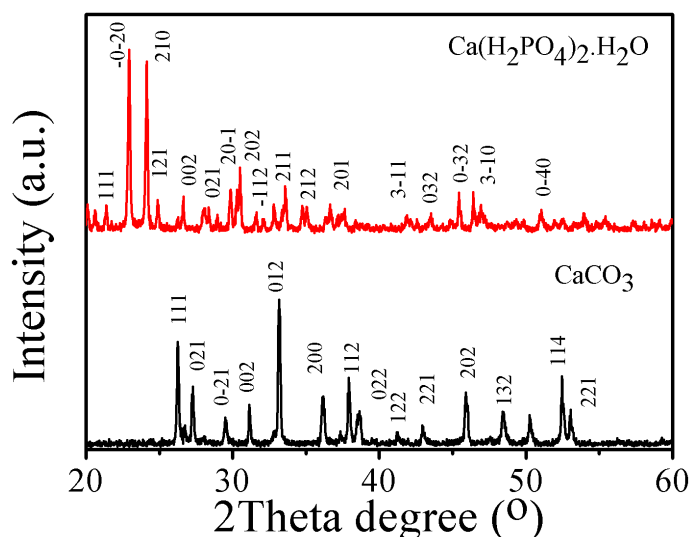


Figure 3: XRD patterns of the as-synthesized CaCO_3 and $\text{Ca}(\text{H}_2\text{PO}_4)_2 \cdot \text{H}_2\text{O}$.

The FT-IR spectra of the as-synthesized CaCO_3 and $\text{Ca}(\text{H}_2\text{PO}_4)_2 \cdot \text{H}_2\text{O}$ products are presented in Figure 4. FTIR spectrum of the as-synthesized CaCO_3 shows fundamental vibration of CO_3^{2-} anion as block unit in CaCO_3 structure[37]. An appeared strong absorption peak of CO_3^{2-} at 1470 cm^{-1} corresponds to the asymmetric stretching mode of $\nu_3\text{-CO}_3$ calcite and vaterite. A observed weak absorption peak at 1070 cm^{-1} is assigned to the symmetric stretching mode of $\nu_1\text{-CO}_3$ calcite and vaterite. A strong and a weak absorption peaks appeared at 854 and 706 cm^{-1} are assigned to $\nu_2\text{-CO}_3$ aragonite and $\nu_4\text{-CO}_3$ calcite, respectively. The FTIR results indicate that the as-synthesized CaCO_3 sample is the mixing of three calcium carbonate phases, which are consistent with XRD results. FTIR spectrum of the as-synthesized $\text{Ca}(\text{H}_2\text{PO}_4)_2 \cdot \text{H}_2\text{O}$ shows fundamental vibrational modes of the subunits in the structure, namely the $[\text{H}_2\text{PO}_4]^-$ ion and H_2O units[37, 38]. The strong bands in the region of $1100\text{--}900 \text{ cm}^{-1}$ are attributed to the P–O stretching vibrations. The bending OPO vibrations appear in the region of $600\text{--}450 \text{ cm}^{-1}$. The couple bands at 1230 and 854 cm^{-1} are assigned to the out-of-plane and in-plane bending modes of P–O–H, respectively. The band around 949 cm^{-1} could be due to either the γ_{OH} (P–OH out-plane bending) or to the P–O stretching vibration. The weak band at about 676 cm^{-1} is due to the rocking mode of the water libration, which appears broaden band than those of the individual ones. The multiple bands in the

O–H stretching mode region are characteristic for the acid salts[38], which appear as ABC trio bands at about 3200-3100 cm^{-1} (A band), 2400–2300 cm^{-1} (B band) and 1860-1680 cm^{-1} (C band). The ν_{OH} stretching modes of HOH in $\text{Ca}(\text{H}_2\text{PO}_4)_2 \cdot \text{H}_2\text{O}$ appeared at 3460 cm^{-1} (ν_3 ; B_2) and 3100 cm^{-1} (ν_1 ; A_1). A broad band at 1650 contribute both to the C band and to water bending mode (ν_2 , A_1 ; H_2O).

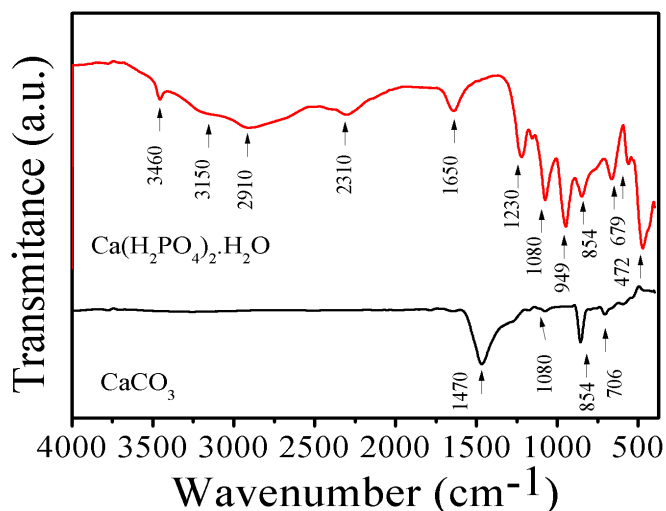


Figure 4: FTIR spectra of the as-synthesized CaCO_3 and $\text{Ca}(\text{H}_2\text{PO}_4)_2 \cdot \text{H}_2\text{O}$.

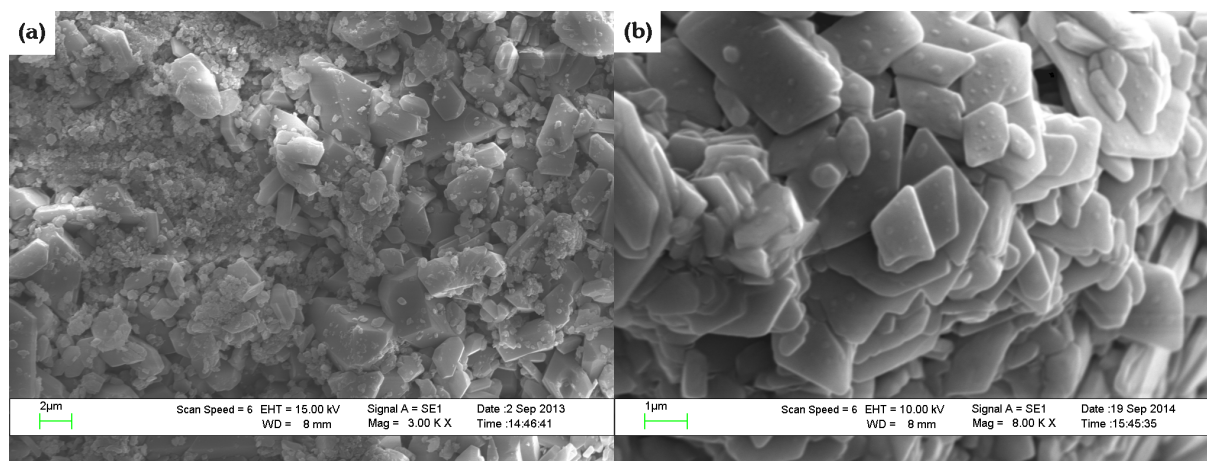


Figure 5: SEM micrographs of the as-synthesized CaCO_3 (a) and $\text{Ca}(\text{H}_2\text{PO}_4)_2 \cdot \text{H}_2\text{O}$ (b).

The SEM micrographs of the as-synthesized CaCO_3 and $\text{Ca}(\text{H}_2\text{PO}_4)_2 \cdot \text{H}_2\text{O}$ powders are shown in Figure 5. The SEM micrograph of the as-synthesized CaCO_3 (Figure 5a) illustrates coalescence in aggregates of non-uniform polyhedral grains of different small and some large sizes and roughness on its surface. The SEM micrograph of the as-synthesized $\text{Ca}(\text{H}_2\text{PO}_4)_2 \cdot \text{H}_2\text{O}$ (Figure 5b) shows coalescence in aggregates of irregularly plate-like shaped crystals of different sizes in the range of 0.40-2.0 μm and flakes on its surface. The morphologies of the as-prepared CaCO_3 and $\text{Ca}(\text{H}_2\text{PO}_4)_2 \cdot \text{H}_2\text{O}$ particles may indicate further nucleation/growth of the nanocrystals inside the powder [1, 15, 24]. The exact particle nucleation and growth mechanisms are occurred by many factors of preparations of general materials, which are not yet clear discussion now. For the as-synthesized samples of this work, the morphologies may be affected by raw material and prepared condition.

Conclusion

Calcium carbonate (CaCO_3) with three mixed phases was successfully obtained by a fast simple, low-cost, and environmentally benign preparation from green mussel shells (a low-cost, enormous waste and abundant natural resource) and was used to prepare monocalcium phosphate monohydrate ($\text{Ca}(\text{H}_2\text{PO}_4)_2 \cdot \text{H}_2\text{O}$). The obtained result indicates that the as-prepared CaCO_3 sample is predominantly of vaterite phase with minor percentages of calcite and aragonite estimated by Kontoyannis and Vagenas equation and the $\text{Ca}(\text{H}_2\text{PO}_4)_2 \cdot \text{H}_2\text{O}$ is pure anorthic phase, revealed by XRD and FTIR. Thermal decomposition of the as-prepared CaCO_3 and $\text{Ca}(\text{H}_2\text{PO}_4)_2 \cdot \text{H}_2\text{O}$ samples related to decarboxylation reaction and dehydration and deprotonation hydrogen phosphate reactions,

respectively, revealed by TGA. The morphologies of the as-prepared CaCO₃ and Ca(H₂PO₄)₂•H₂O particles appear different non-uniform of irregularly plate-like shaped crystals, revealed by SEM. The preparation method has a great potential to be used in industry for large scale production of CaCO₃ and Ca(H₂PO₄)₂•H₂O from green mussel shells, enormous garbage and abundant natural resource for various applications.

Acknowledgements-This work would like to acknowledge the financial support from the Faculty of Science, King Mongkut's Institute of Technology (KREF#25600105067)

References

1. A.A. Francis, M.K. Abdel Rahman, *J. Clean. Prod.* 137 (2016) 1432-1438.
2. K. Fukui, N. Arimitsu, S. Kidoguchi, T. Yamamoto, H. Yoshida, *J. Hazard. Mater.* 163(1) (2009) 391-395.
3. P. Leelatawonchai, T. Laonapakul, *Adv. Mater. Res.* 931-932 (2014) 370-374.
4. S. Jinawath, D. Pongkao, W. Suchanek, M. Yoshimura, *Inter. J. Inorg. Mater.* 3(7) (2001) 997-1001.
5. F.K. Cameron, J.M. Bell, *J. Amer. Chem. Soc.* 28(9) (1906) 1222-1229.
6. W. Habraken, P. Habibovic, M. Epple, M. Bohner, *Mater. Today* 19(2) (2016) 69-87.
7. N. Lertcumfu, P. Jaita, S. Manotham, P. Jarupoom, S. Eitssayeam, K. Pengpat, G. Rujijanagul, *Ceram. Inter.* 142(9) (2016) 10638-10644.
8. I. Zarkesh, M.H. Ghanian, M. Azami, F. Bagheri, H. Baharvand, J. Mohammadi, M.B. Eslaminejad, *Colloids Surf. B-Biointerfaces* 157 (2017) 223-232.
9. J.H. Shariffuddin, M.I. Jones, D.A. Patterson, *Chem. Eng. Res. & Des.* 91(9) (2013) 1693-1704.
10. K. Nasri, H. El Feki, P. Sharrock, M. Fiallo, A. Nzihou, *Ind & Eng. Chem. Res.* 54(33) (2015) 8043-8047.
11. S.V. Dorozhkin, *Mater.* 2(2) (2009) 399-498.
12. F. Bennani, M. Badraoui, M. Mikou, *J. De Phys. Iv* 123 (2005) 159-163.
13. G.S. Kumar, E.K. Girija, M. Venkatesh, G. Karunakaran, E. Kolesnikov, D. Kuznetsov, *Ceram. Inter.* 43(3) (2017) 3457-3461.
14. M.C. Barros, P.M. Bello, M. Bao, J.J. Torrado, *J. Clean. Prod.* 17(3) (2009) 400-407.
15. B. Boonchom, *J. Alloys Compds.* 482(1-2) (2009) 199-202.
16. C. Combes, C. Rey, *Acta Biomater.* 6(9) (2010) 3362-3378.
17. Y.M. Hsu, C.Y. Wu, D.A. Lundgren, J.W. Nall, B.K. Birky, *J. Occup. Environ. Hyg.* 4(1) (2007) 17-25.
18. R.Z. LeGeros, S. Lin, R. Rohanizadeh, D. Mijares, J.P. LeGeros, *J. Mater. Sci.: Mater. Med.* 14(3)(2003)201-209
19. E. Boanini, M. Gazzano, A. Bigi, *Acta Biomater.* 6(6) (2010) 1882-1894.
20. S.V. Dorozhkin, *Acta Biomater.* 6(3) (2010) 715-734.
21. R. Emadi, S.I.R. Esfahani, F. Tavangarian, *Mater. Lett.* 64(8) (2010) 993-996.
22. K. Fukui, S. Kidoguchi, N. Arimitsu, K. Jikihara, T. Yamamoto, H. Yoshida, *J. Env. Manag.* 90(8) (2009) 2709-2714.
23. R. Ghosh, R. Sarkar, *Mater. Sci. Eng. C* 67 (2016) 345-352.
24. C.K. Hsu, *Mater. Chem. Phys.* 80(2) (2003) 409-420.
25. Y.H. Hsu, I.G. Turner, A.W. Miles, *Bioceram.* Vol 172005, pp. 305-308.
26. C. Huang, P. Cao, *Mater. Chem. Phys.* 181 (2016) 159-166.
27. I.J. Macha, L.S. Ozyegin, J. Chou, R. Samur, F.N. Oktar, B. Ben-Nissan, *J. Austr. Ceram. Soc.* 49(2013)122-128
28. M. Sari, Y. Yusuf, *Inter. J. Nanoelect. Mater.* 11(3) (2018) 357-369.
29. J. Sanchez-Enriquez, J. Reyes-Gasga, *Ultra. Sonochem.* 20(3) (2013) 948-954.
30. A. Shavandi, A.E.D. A. Bekhit, A. Ali, Z. Sun, J.T. Ratnayake, *Powd. Tech.* 273 (2015) 33-39.
31. Y. Yang, Q. Yao, X. Pu, Z. Hou, Q. Zhang, *Chem. Eng. J.* 173(3) (2011) 837-845.
32. H. Onoda, S. Yamazaki, *J. Asian Ceram. Soc.* 4(4) (2016) 403-406.
33. K.N. Islam, M.Z.B.A. Bakar, M.E. Ali, M.Z.B. Hussein, M.M. Noordin, M.Y. Loqman, G. Miah, H. Wahid, U. Hashim, *Powd. Tech.* 235 (2013) 70-75.
34. A.I. Iotescu, G. Vlase, T. Vlase, N. Doca, *J. Therm. Anal. Calorim.* 88(1) (2007) 121-125.
35. Z. Zyman, A. Goncharenko, D. Rokhmistrov, *J. Cryst. Growth* 478 (2017) 117-122.
36. C.G. Kontoyannis, N.V. Vagenas, *Analyst* 125 (2000) 251-255.
37. C.K. Hsu, *Thermochim. Acta* 392 (2002) 157-161.
38. J. Xu, D. F.R. Gilson, I. S. Butler, *Spectrochim. Acta Part A: Mol. Biomol. Spec.* 54(12) (1998) 1869-1878.

(2019) ; <http://www.jmaterenvirosci.com>